Journal of the Ceramic Society of Japan 122 [4] 260-266 2014 Paper

Phase formation of $BaTiO_3$–$Bi(Zn_{1/2}Ti_{1/2})O_3$ perovskite ceramics

Narit TRIAMNAK, Geoff L. BRENNECKA,* Harlan J. BROWN-SHAKLEE,* Mark A. RODRIGUEZ* and David P. CANN

Materials Science, School of Mechanical, Industrial, and Manufacturing Engineering, Oregon State University, Corvallis, Oregon 97331 USA

***Materials Science and Engineering Center, Sandia National Laboratories, Albuquerque, NM 87185–1411 USA**

Materials based on BiMO$_3$-modified $BaTiO_3$ have been shown to exhibit a number of attractive electrical and electromechanical properties. In addition, many of the materials in this broad family exhibit reduced sintering temperatures for densification as compared to pure $BaTiO_3$. We report here a study of the phase evolution and sintering behavior of $Bi(Zn_{1/2}Ti_{1/2})O_3$-modified $BaTiO_3$ materials from low-cost mixed oxide/carbonate precursor powders. By accelerating the reaction of the $BaCO_3$ species and increasing the diffusion kinetics associated with densification, $Bi(Zn_{1/2}Ti_{1/2})O_3$ additions reduce the calcination and sintering temperatures by ~200°C compared to unmodified $BaTiO_3$. This system provides an example of the important and often overlooked role of additives in the calcination, phase evolution, and densification processes, and provides insight into mechanisms that may be further exploited in this and other important materials systems. We are quite honored to have the opportunity to publish in a special issue dedicated to the life and work of our dear late colleague Prof. Marija Kosec. The topic of this paper is fitting as well, since the work was in large part directly inspired by her work on the importance of reactions and intermediate phases in the alkali niobate systems[1)–4)] and heavily informed by her work on the Pb-based perovskites.[5),6)] Marija appreciated better than most the importance of careful processing in the formation of fine ceramics, and the global ceramics community is grateful to her for all of the lessons that she taught us—and through her papers and her students, continues to teach us.

Key-words : Phase evolution, Relaxor, Diffraction, Perovskite

[Received December 1, 2013; Accepted February 18, 2014]

1. Introduction

Modifications to $BaTiO_3$ with BiMO$_3$-type perovskite end members, where M represents any number of single or charge-balancing pairs of transition metals such as Fe, Sc, In, Zn + Ti, Mg + Ti, and others, have received increasing attention in recent years in efforts to find replacements for Pb-containing materials, particularly for applications requiring high-operating temperatures. $BaTiO_3$ itself is the prototype ferroelectric, exhibiting large permittivity ($\varepsilon_r > 1000$), reasonably large and easily switchable spontaneous polarization, and high mechanical quality factor. Much of the incredible success of the multilayer ceramic capacitor (MLCC) industry has been directly related to the ability to tailor the dielectric properties of $BaTiO_3$-based materials through extensive chemical modifications designed to broaden the phase transitions across application-relevant temperature ranges, improve the temperature stability of dielectric properties, and compensate for processing atmosphere induced point defects.

Currently, application drivers are pushing for higher operating temperature capabilities while environmental policies increasingly limit the use of Pb-containing materials. Thus, finding ways to increase the maximum operating temperature of $BaTiO_3$-based materials has become an important area of research. Perovskites with Bi-additives have been studied nearly as long as $BaTiO_3$ itself[7),8)] and in fact, Bi-containing additives were part of the trade secrets of high voltage ceramic capacitors developed in the 1970s. However, the pioneering work of Eitel et al. was the first study that systematically investigated a variety of BiMO$_3$ perovskite end member systems with the goal of increasing operating temperature capabilities.[9)] Since then, a number of studies[10)–15)] have demonstrated the impressive properties, both electrical and electromechanical, that can be obtained from this family of materials, often without any additional compensatory doping and/or process optimization. One of the more intriguing aspects of these systems (and one that is often noted in casual conversations among researchers working on these materials, but not often reported in modern literature) is how resilient they appear to be to relatively large changes in processing parameters that would, in many other electroceramic systems, result in dramatic changes in electrical properties. Confirmation of this resiliency comes from inspection of the widely varying processing parameters with similar resulting relaxor behavior reported by multiple groups across the world working with, in particular, $Bi(Zn_{0.5}Ti_{0.5})O_3$ or $Bi(Mg_{0.5}Ti_{0.5})O_3$ modified $BaTiO_3$. While the near-ambient properties are indeed similar for Bi and Zn (or Mg) doped $BaTiO_3$, the dielectric behavior above 250°C appears to be highly processing and chemistry sensitive. Insensitivity to processing conditions is attractive from a manufacturing standpoint because of relaxed process-control requirements, but understanding the underlying mechanism(s) is critical to optimize the performance, particularly at high temperatures, through a mechanistic understanding of phase and microstructure evolution.

It is well known from both bulk polycrystalline and thin film studies that the stability of $BaCO_3$ (and related oxycarbonate derivatives) is critical during the processing of $BaTiO_3$-based materials in air.[16)–18)] In addition, during the synthesis of Bi-based perovskites, a number of intermediate or secondary phases have

† Corresponding author: G. L. Brennecka; E-mail: glbrenn@sandia.gov

‡ Preface for this article: DOI http://dx.doi.org/10.2109/jcersj2.122.P4-1

DOI http://dx.doi.org/10.2109/jcersj2.122.260

been observed, often exhibiting a pyrochlore or fluorite structure. The pyrochlore structure, generically represented as $A_2B_2O_7$, is extremely tolerant to substitution on both the A and B cation sites as well as to vacancies on any or all of the sites. In the Pb-based analogues, pyrochlore phases can either be unavoidable but manageable transient intermediate phases[19)–21)] or deep thermodynamic minima from which the perovskite phase cannot be recovered through thermal means alone.[22)] Importantly, despite the frequent observation of intermediate pyrochlore phases in the processing of bismuth-based perovskites, $Bi_2Ti_2O_7$ has been found not to be a thermodynamically stable phase at relevant sintering temperatures.[23),24)] Instead, the majority of the Bi_2O_3–TiO_2 phase diagram consists of mixtures of the Aurivillius-family $Bi_4Ti_3O_{12}$ layered perovskite phase and either $Bi_2Ti_4O_{11}$ or $Bi_{12}TiO_{20}$.[25)–29)]

The $Bi_4Ti_3O_{12}$ phase has been observed as a secondary phase in simple perovskite systems with Bi concentrations beyond the solubility limit[30),31)] and as a transient intermediate phase during the mixed-oxide processing of Bi- and Ti-containing perovskite materials.[32)] Given the importance of intermediate phase development and solid state reactions among precursors to the phase, chemical distribution, and properties of the resultant ceramics, detailed study of the reactions involved in the processing of materials in the $BaTiO_3$–Bi$M$$O_3$ systems is needed. In this work, we focus on the $BaTiO_3$–$Bi(Zn_{1/2}Ti_{1/2})O_3$ (BT–BZT) system, and in particular, the effects of BZT additions on the phase formation and densification relative to pure $BaTiO_3$.

Huang et al. studied the solubility limit and dielectric properties of this binary solid solution.[12)] They observed that the solubility limit of BT–BZT was approximately ~34% BZT as determined by ex situ powder diffraction. The phase transition associated with the $BaTiO_3$ Curie temperature (T_C) was also shown to decrease in temperature and sharpness with increasing BZT additions up to ~10%.[12),13)] Materials with >10% BZT substitution exhibited relaxor behavior with broad, frequency-dependent maxima in both relative permittivity and loss, a slim Polarization vs. Electric Field response, and large field-stable permittivity values which can exceed 1000 even under electric fields exceeding 100 kV/cm. Very similar phase stability and electrical properties have been reported for BT-BMT ceramics.[31)]

2. Experimental methods

In this study, solid solutions of 0.80BT–0.20BZT, 0.85BT–0.15BZT, and pure BT were prepared by a conventional solid-state method. Commercially available powders of Bi_2O_3 (≥99.9%), ZnO (≥99.9%), TiO_2 (≥99%), and $BaCO_3$ (≥99.8%) were used as starting materials. The powders were subjected to X-ray diffraction (XRD), weighed in the appropriate stoichiometric amounts, mixed in 100% ethanol, vibratory or ball milled with yttrium-stabilized zirconia media for 6 h, and then dried in 75°C ovens. Some powders were separated at this point for in situ diffraction experiments; the rest of the powders were calcined in covered crucibles followed by additional milling and drying.

Two different XRD techniques were used to track phase evolution of the bismuth and zinc doped dielectric powders. Diffraction patterns of the 0.85BT–0.15BZT and BT specimens were collected at room temperature using a Bruker-AXS D8. In situ high temperature XRD experiments were performed using a Scintag PAD X diffractometer (Thermo Electron Inc.; Waltham, MA). This diffractometer was equipped with a sealed-tube source (Cu Kα, $\lambda = 0.15406$ nm), an incident-beam mirror optic, a peltier-cooled Ge solid-state detector, and a Buehler hot-stage with Pt/Rh heating strip and surround heater. Scintag instrument power settings were 40 kV and 30 mA, and fixed slits were employed. Temperature calibration was performed using thermal expansion behavior of known materials (e.g., alumina) and calibrated to ±5°C. Samples were heated in a static air environment atop Pt foil on an Al_2O_3 setter using a 20°C/min ramp rate to the desired analysis temperature. Diffraction patterns were collected over a scan range of 20–60° 2θ at a step-size of 0.05° 2θ and a count time of 3 s. Typical collection time for each scan was ~40 min.

Powders calcined to 900°C (BT–BZT) or 1100°C (BT) and found to be phase-pure were mixed with 3 wt % polyvinyl butyral binder and consolidated into discs under 150 MPa uniaxial pressure. The green pellets were heated to 400°C for 3 h in a covered Al_2O_3 crucible for binder burnout, and then ramped at 3°C/min to a sintering temperature between 500–1400°C with a 2 h hold time at and a cooling rate of 5°C/min. The radial shrinkage of each pellet was measured after sintering. Pellets for dilatometer measurements were consolidated under 100 MPa uniaxial pressure and then pressed to 350 MPa under isostatic pressure. These green pellets underwent binder burnout and 10°C/min sintering in a dilatometer using Al_2O_3 push rods. All processing and characterization steps were carried out in air.

3. Results and discussion

As a baseline for comparison, XRD patterns of BT powders after cooling from different calcination temperatures are illustrated in **Fig. 1**. At a calcination temperature as low as 500°C, as shown in Fig. 1(a), the XRD data of the calcined powders showed no changes compared to the XRD pattern of the reagent powders, which is not shown here. Only $BaCO_3$ (**B**) and TiO_2 (**T**) peaks were observed which matched JCPDS file numbers 00-045-1471 and 00-021-1272, respectively. The perovskite $BaTiO_3$ phase (*) initially appeared after calcination at 600°C, with the dominant reflection attributed to the (110) peak at 2θ~31.5°. The progression of the calcination reactions with increasing calcination temperature is evidenced by the gradual decrease of intensity of the $BaCO_3$ (**B**) and TiO_2 (**T**) reflections as intensities of the BT (*) reflections increased. After calcination at 950°C, the reflections from the $BaCO_3$ (**B**) and TiO_2 (**T**) phases could not be seen in the XRD data.

There have been prior reports of the co-existence of a Ba_2TiO_4 phase[33),34)] as a secondary phase in the formation of BT. This phase can be seen in the data in Fig. 1(a) from the peak at 2θ~28.5° over temperature range of 700–950°C. However, it is clearly seen in Fig. 1(b) that multiple phases coexist (@) over this range in calcination temperatures. Therefore, a slow scan XRD at an increment of 0.001° and a scan speed of 0.5° per minute was carried out from $2\theta = 23$ to 33° in order to identify the multiple phases. Interestingly, a $BaTi_2O_5$ phase (**X**), matched with JCPDS file number 00-034-0133, was initially observed at calcination temperatures between 700–800°C, as shown in Fig. 1(c). As the temperature increased, two polymorphs of the stoichiometry Ba_2TiO_4 were observed over temperature range 750–950°C. The first phase (**W**), which was seen between 750–900°C, is matched with JCPDS file number 01-072-0135, and the second (**M**), matched with JCPDS file number 00-038-1481, was seen between 850–950°C. Finally, the complete tetragonal perovskite phase of BT, matched with JCPDS file number 01-081-2204, was observed after cooling from a calcination temperature of 1100°C.

According to the XRD data, the reaction sequence of the phase formation in BT can be represented by two reactions as follows;

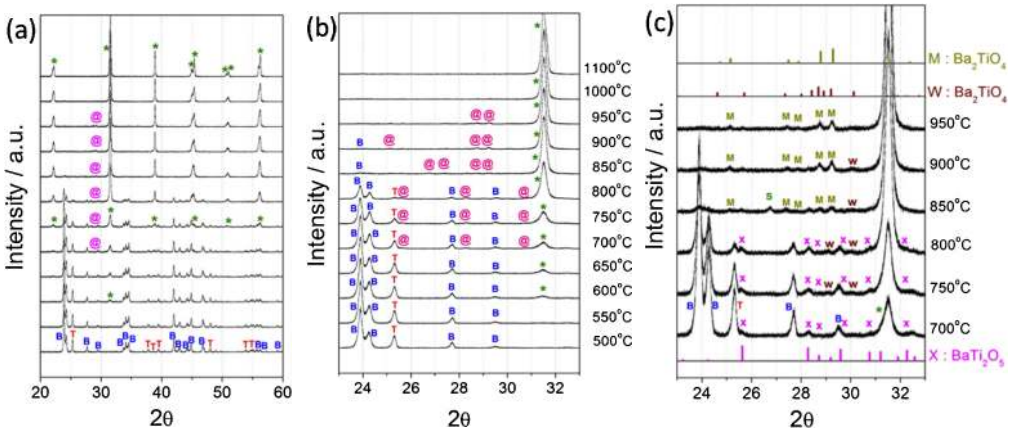

Fig. 1. X-ray diffraction patterns of calcined BT powder after various calcination temperatures. B = $BaCO_3$ (orthorhombic), T = TiO_2, * = perovskite phases, @ = multiple phases, X = $BaTi_2O_5$, W = Ba_2TiO_4, M = Ba_2TiO_4, S = $BaCO_3$ (rhombohedral, stabilized).

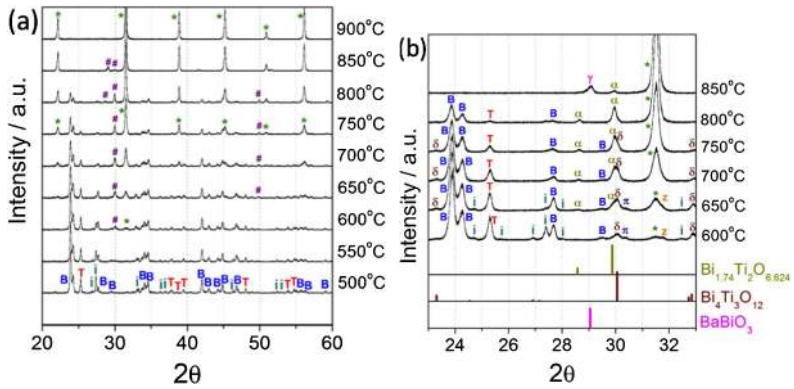

Fig. 2. X-ray diffraction patterns of calcined 0.85BT–0.15BZT powders after various calcination temperatures. B = $BaCO_3$, T = TiO_2, i = Bi_2O_3, Z = ZnO, * = perovskite phases, # = multiple phases, π = unknown, $\delta = Bi_4Ti_3O_{12}$, $\alpha = Bi_{1.74}Ti_2O_{6.624}$, and $\gamma = BaBiO_3$.

$$BaCO_3 + 2TiO_2 \xrightarrow{700-800^\circ C} BaTi_2O_5 + CO_2$$

$$BaTi_2O_5 + BaCO_3 \xrightarrow{700-800^\circ C} 2BaTiO_3 + CO_2$$

and

$$2BaCO_3 + TiO_2 \xrightarrow{750-950^\circ C} Ba_2TiO_4 + 2CO_2$$

$$Ba_2TiO_4 + TiO_2 \xrightarrow{750-950^\circ C} 2BaTiO_3$$

For comparison to the phase evolution of pure $BaTiO_3$, **Fig. 2** shows the XRD patterns of 0.85BT–0.15BZT powders after cooling from 2 h holds at various calcination temperatures. As with pure BT, the XRD data for the 500°C calcined powder showed no evidence of the onset of phase changes. The phases that existed at 500°C included $BaCO_3$ (**B**), Bi_2O_3 (**i**), TiO_2 (**T**) and ZnO (**Z**) reagent phases which correspond to JCPDS file numbers 00-045-1471, 00-041-1449, 00-021-1272, and 00-036-1451, respectively. It should be noted that even though the ZnO peaks are not clearly visible in Fig. 2(a) due to low atomic number and relatively small volume fraction, the main peak (100) at 2θ~31.7° is visible upon closer inspection [Fig. 2(b)]. The perovskite phase (*****), identified from the (110) reflection at 2θ~31.5° as shown in Fig. 2(a), was first observed after calcination at 600°C, the same temperature at which it was first observed for pure $BaTiO_3$. However, phase-pure BT–BZT perovskite was obtained at a calcination temperature of 900°C, which is 200°C lower than for the case of pure BT.

No evidence of intermediate $BaTi_2O_5$ or Ba_2TiO_4 phases was observed in the BT–BZT calcination studies; instead, a number of intermediate Bi-containing phases [collectively identified by **#** in Fig. 2(a)] were present. A slow scan XRD was investigated again from $2\theta = 23$ to 33° and the results are illustrated in Fig. 2(b). After a low calcination temperature of 600°C, a pyrochlore phase $Bi_4Ti_3O_{12}$ (**δ**) (JCPDS file number 00-035-0795) and a weak unknown phase identified as (**π**) were observed in the data. Their peak intensities decreased as the calcination temperature increased, finally disappearing within the detection limits of XRD at temperatures of 700 and 800°C, respectively. Another pyrochlore phase with the stoichiometry $Bi_{1.74}Ti_2O_{6.624}$ (**α**) was observed at 650°C. The volume fraction of the $Bi_{1.74}Ti_2O_{6.624}$ (**α**) phase, as inferred from the intensity of the (311) peak at 2θ~28.6°, increased with an increase in the calcination temperature until it suddenly decreased after a calcination temperature of 850°C. By increasing the temperature further, the $Bi_{1.74}Ti_2O_{6.624}$ (**α**) phase disappeared within the detection limits of XRD. In addition, an unexpected perovskite phase based on $BaBiO_3$ (**γ**), with a strong peak at 2θ~29° was detected after calcination at 850°C.

To further investigate the curious phase evolution of the BT–BZT materials, two additional studies were conducted. Focusing on the rather distinct differences observed between the sample calcined for 2 h at 800°C and the one calcined for 2 h at 850°C, powders of 0.85BT–0.15BZT were calcined at a temperature

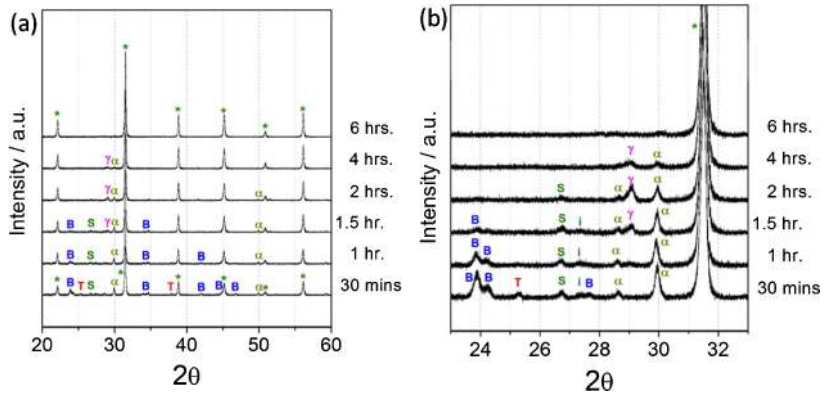

Fig. 3. X-ray diffraction patterns of 0.85BT–0.15BZT powders after calcination at 850°C for various times. B = $BaCO_3$, T = TiO_2 or $Ba_{0.2}Bi_{0.8}TiO_{2.5}$, i = Bi_2O_3, S = potential $BaCO_3$, * = perovskite phases, α = $Bi_{1.74}Ti_2O_{6.624}$ or Bi_2O_3 (stabilized), and γ = $BaBiO_3$ (ss).

of 850°C for various soaking times ranging from 30 min to 6 h. In addition, in situ diffraction studies were carried out during heating of 0.80BT–0.20BZT powders from 25 to 850°C.

Figure 3 illustrates the XRD patterns of mixed 0.85BT–0.15BZT powders following calcination at 850°C for various soaking times. Peaks that suggest residual precursor species ($BaCO_3$, Bi_2O_3, and TiO_2) are clearly seen after 30 min at 850°C; their intensities gradually decrease with extended calcination times but persist even after 1.5 h at 850°C. Evidence of a pyrochlore phase $Bi_{1.74}Ti_2O_{6.624}$ (~30° 2θ) was also clearly present in the early stages, but the intensity of this peak decreased as the calcination time increased, and its presence was no longer observed after calcination for 6 h. An alternate hypothesis for the peak at ~30° 2θ is the persistence of Bi_2O_3 in a chemically stabilized high temperature form (JCPDS 01-080-894). Pyrochlore formation would be consistent with the lead-based analogous compounds, and would indicate that the $Bi_{1.74}Ti_2O_{6.624}$ phase is an intermediate phase that reacts with the remaining precursors in order to form the resultant perovskite BT–BZT solid solution.

A peak at ~26.7° appears early in the calcination studies at 850°C, but gradually disappears as $BaBiO_3$ appears with increased calcination times. This peak can be indexed as a (002) reflection from a $BaCO_3$ orthorhombic cell with ~1% tensile strain, but unambiguous identification is not possible from this data alone.

The phase fraction of $BaBiO_3$, a perovskite that exhibits a mixture of Bi^{3+} and Bi^{5+} valence states, reached its maximum concentration after 2 h of calcination time but then decreased following longer calcination times. This $BaBiO_3$ supercell perovskite exhibits cell contraction that is likely due to Bi substitution on the Ba site and possibly even Zn occupancy on the Bi site. This phase was labeled $BaBiO_3$ (ss) in Fig. 3 to denote the strong possibility of a Bi-rich and Zn containing phase.

While these ex situ studies permitted laboratory measurement with excellent signal to noise resulting from high sampling statistics, they may not have captured actual phase evolution because unquenchable phases and reactions outside of the calcination process are unobservable at room temperature. Thus, complementary in situ diffraction data were also collected during heating of the mixed powders, and are shown in **Fig. 4**. Many of the minor phases observed in the ex situ diffraction studies are not observed here because they formed during cooling of the ex situ samples or, presumably, because the reduced counting statistics in the in situ experimental conditions prevents them from being observed above the background. The overall phase evolution and progression, however, is consistent between the two data series. The precursor powders began to react somewhere around 500°C, apparently starting with the decomposition of Bi_2O_3 and the formation of one or more bismuth titanate species (i.e., $Bi_4Ti_3O_7$ and/or $Bi_{1.74}Ti_2O_{6.624}$) before the $BaCO_3$ began to degrade above 700°C, the same temperature at which the $BaCO_3$ began to degrade in the pure $BaTiO_3$ system. In the BT–BZT system, there was no evidence of the presence of $BaCO_3$ after 2 h of calcination at 900°C, while in pure $BaTiO_3$, faint $BaCO_3$ peaks persisted until calcination at 950°C. More importantly, however, BT–BZT samples were completely single phase to the resolution of our diffraction after calcination at 900°C for 2 h (or 850°C for 6 h) whereas pure $BaTiO_3$ required heating to at least 1100°C for 2 h for elimination of all detectable secondary phases. Formation of intermediate phases that are closely related to the perovskite structure (e.g., $Bi_4Ti_3O_{12}$, $BaBiO_3$) presumably lowered the energy barrier for this final conversion, and may help to explain the reduced temperatures required to achieve single phase perovskite BZT-modified materials.

In addition to providing confirmation of the general phase evolution observed via the ex situ studies, these in situ measurements enabled the unambiguous identification of the peak at ~26.7° as a $BaCO_3$ (002) reflection. $BaCO_3$ undergoes a reversible phase transition from the low temperature orthorhombic (*Pmcn*) form to the high temperature rhombohedral (*R3m*) form around 811°C[35] which is associated with a 2.8% change in volume. Both this transition strain and the highly anisotropic thermal expansion (visible in Fig. 4) are concentrated along the *c* axis of the $BaCO_3$ unit cell. From the in situ data, it can be seen that the peak in the vicinity of 27° at 500°C is clearly the $BaCO_3$ (002) peak. We speculate that the reverse transformation ($BaCO_{3,\ rhombohedral}$ to $BaCO_{3,\ orthorhombic}$) is hindered during cooling for the powders used for ex situ measurements. It is also possible that any partially-reacted $BaCO_3$ species is mechanically strained after cooling due to interdiffusion during the formation of the other observed phases, all of which have significantly lower coefficients of thermal expansion than either $BaCO_3$ phase. Upon cooling from 850°C, one or both of these factors result in an orthorhombic $BaCO_3$ unit cell which is expanded by roughly 1% along the *c* axis, leading to a diffraction peak at 26.7° 2θ, as seen in Fig. 3.

Another important feature of these data is that the persistence of $BaCO_3$ promotes the formation of bismuth rich (relative to the

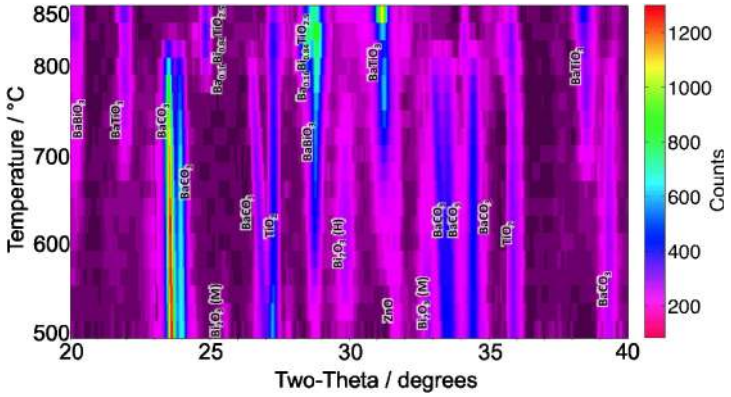

Fig. 4. Diffraction patterns from in situ measurements. Two Bi_2O_3 phases were identified: (M) room temperature monoclinic and (H) a high temperature form. Continuity of peaks also enabled the identification of the S peak from Fig. 3 as $BaCO_3$.

target perovskite composition) compounds. These bismuth-rich intermediate compounds must thermally degrade in the presence of reactive barium compounds to produce the targeted terminal perovskite composition. The formation of phase-pure Bi- and Zn- co-doped $BaTiO_3$ is therefore a complex multistep reaction sequence. The aforementioned energy barriers that contribute to Bi-rich compounds appear to be strongly linked to the relatively slow decomposition of $BaCO_3$. Keeping in mind that even materials that appear to be single phase via XRD may exhibit non-random cation distribution(s), it is also speculated that these intermediate phases may play a role microstructure development within sintered ceramics of these materials.

Analogous to the diffraction studies, densification of these materials was studied using two complementary approaches. Cylindrical pellets of BT and 0.85BT–0.15BZT were sintered for 2 h at different temperatures, and their shrinkage following this treatment was monitored through geometric measurements. In addition, dilatometry experiments were carried out on $BaTiO_3$ and 0.80BT–0.20BZT pellets for in situ monitoring of shrinkage during the sintering process. Data from these combined studies are summarized in **Fig. 5**.

From the ex situ shrinkage measurements, it is clear that the addition of BZT into BT has the effect of lowering the sintering temperature by approximately 200 to 300°C. While the sintering temperature of BT is about 1400°C, 0.85BT–0.15BZT samples reached full density at temperatures as low as 1100°C. The shapes of the shrinkage curves for both materials are very similar. It is interesting to note that the onset of sintering in the 0.85BT–0.15BZT composition occurred at 600°C. Given that the XRD data on the starting powder indicated phase pure pseudo-cubic perovskite, the low temperature shrinkage may be indicative of the influence of a glassy or poorly crystalline phase. From the in situ dilatometer data, it is similarly clear that the BT–BZT sample densified at a significantly lower temperature than the pure $BaTiO_3$, though the temperature difference is not quite as large as in the ex situ situation. While evidence of densification does start to appear in the dilatometer data as low as ~720°C, the densification rate remains low until >800°C. The additional low-temperature shrinkage observed in the ex situ data with a 2 h hold may be indicative of a small amount of liquid phase-induced consolidation rather than extensive solid state diffusion.

Given the prevalence of intermediate phases in the BT–BZT system, further studies were carried out to investigate the stability of the pseudo-cubic perovskite, once formed, at these intermediate temperatures. After the calcined BT–BZT powders were found to

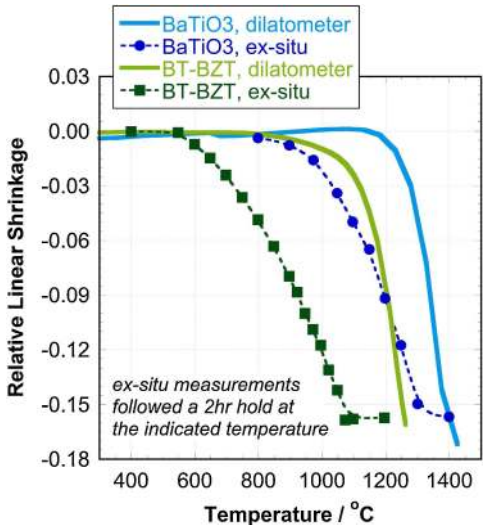

Fig. 5. Linear shrinkage of pure BT and BZT–BT measured via ex situ measurement of shrinkage after 2 h soak times at different temperatures (dotted line) and via in situ measurement of shrinkage by dilatometry (solid line).

be single phase, they were re-heated, both ex situ after consolidation into pellets (0.85BT–0.15BZT) and in situ in powder form (0.80BT–0.20BZT) to investigate the stability of the (pseudo)-cubic perovskite phase in the BT–BZT system. **Figure 6** illustrates the XRD patterns collected at room temperature of 0.85BT–0.15BZT pellets sintered at temperatures between 550–900°C. No noticeable changes were observed in the diffraction patterns, even after extended annealing at temperatures corresponding to the presence of secondary phases observed during the calcination process. Moreover, lattice parameters of these samples, obtained using Cohen's method combined with a least squares method, are shown in **Fig. 7**. A lack of any significant change in lattice parameter with sintering temperature also supports the stability of the cubic perovskite phase that was initially formed after calcination at 850°C for 6 h.

Fully calcined 0.80BT–0.20BZT powders were also reheated in powder form on the diffractometer hot stage, and no further changes in structure or phase content were observed upon heating to 850°C, consistent with the ex situ studies. Collection of this temperature-dependent data also enabled tracking of the lattice parameter from 25 to 850°C, shown in **Fig. 8**, which reveals a

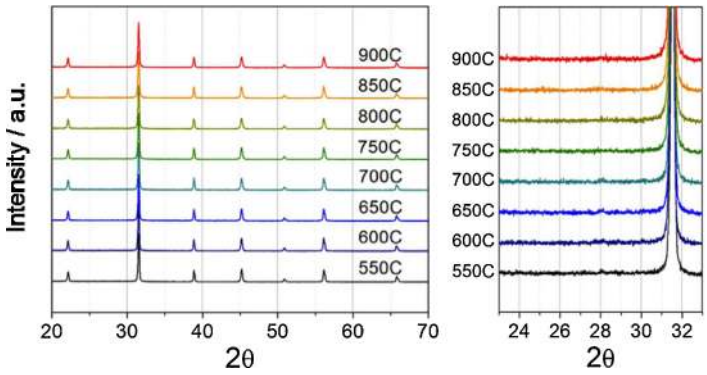

Fig. 6. X-ray diffraction patterns of 0.85BT–0.15BZT pellets after sintering at 550–900°C.

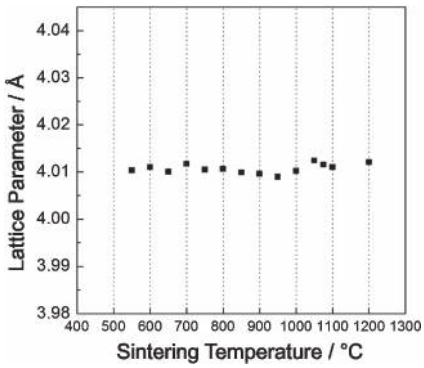

Fig. 7. Room temperature lattice parameter values of 0.85BT–0.15BZT pellets after sintering at various temperatures between 550–1200°C.

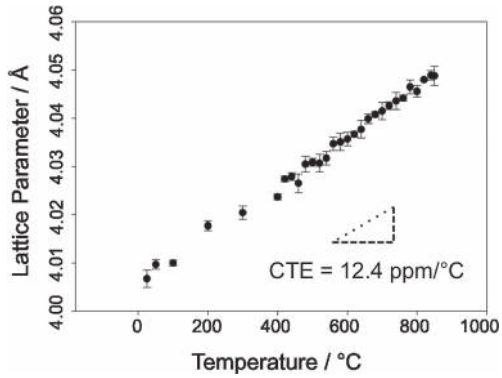

Fig. 8. Lattice parameter values of the single-phase perovskite 0.80BT–0.20BZT powder after calcination collected during re-heating and showing a constant CTE = 12.4 ppm/°C.

constant coefficient of thermal expansion of 12.4 ppm/°C over this temperature range.

4. Conclusions

Intermediate phases strongly influence the phase development of $BaTiO_3$-based materials formed from oxide and carbonate precursors. Additions of $Bi(Zn_{0.5}Ti_{0.5})O_3$, already known to produce ceramics with relaxor dielectric characteristic and attractive voltage- and temperature-stability of dielectric response, dramatically change the sequence and species of intermediate phases formed during calcination. The end result is that powders can be formed which are single phase by XRD at 850°C, more than 200°C lower than pure $BaTiO_3$ from the same starting powders. In addition, densification of pellets formed from these powders began and completed ~200°C below comparable $BaTiO_3$ parts.

Acknowledgements The authors would like to thank James Griego, Tom Chavez, and Mia Blea-Kirby of Sandia National Laboratories for assistance with sample preparation and characterization. The authors gratefully acknowledge the support of Dr. Imre Gyuk and the Department of Energy's Office of Electricity Delivery and Energy Reliability. Sandia National Laboratories is a multiprogram laboratory managed and operated by Sandia Corporation, a wholly owned subsidiary of Lockheed Martin Corporation, for the U.S. Department of Energy's National Nuclear Security Administration under contract DE-AC04-94AL85000.

References

1) T. Rojac, M. Kosec, M. Polomska, B. Hilczer, P. Segedin and A. Bencan, *J. Eur. Ceram. Soc.*, 29, 2999–3006 (2009).
2) T. Rojac, A. Bencan and M. Kosec, *J. Am. Ceram. Soc.*, 93, 1619–1625 (2010).
3) T. Rojac, Z. Trtnik and M. Kosec, *Solid State Ionics*, 190, 1–7 (2010).
4) T. Rojac, B. Malic, M. Kosec, M. Polomska, B. Milczer, B. Zupancic and B. Zalar, *Solid State Ionics*, 215, 1–6 (2012).
5) G. Trefalt, B. Malic, D. Kuscer, J. Holc and M. Kosec, *J. Am. Ceram. Soc.*, 94, 2846–2856 (2011).
6) H. Ursic, J. Tellier, J. Holc, S. Drnovsek and M. Kosec, *J. Eur. Ceram. Soc.*, 32, 449–456 (2012).
7) G. A. Smolenskii, V. A. Isupov and A. I. Agranovskaya, *Sov. Phys. Solid State*, 3, 651–655 (1961).
8) E. C. Subbarao, *J. Chem. Phys.*, 34, 695–696 (1961).
9) R. E. Eitel, C. A. Randall, T. R. Shrout and P. W. Rehrig, *Jpn. J. Appl. Phys.*, 40, 5999–6002 (2001).
10) S. O. Leontsev and R. E. Eitel, *J. Am. Ceram. Soc.*, 92, 2957–2961 (2009).
11) H. Ogihara, C. A. Randall and S. Trolier-McKinstry, *J. Am. Ceram. Soc.*, 92, 110–118 (2009).
12) C. C. Huang and D. P. Cann, *J. Appl. Phys.*, 104, 024117 (2008).
13) N. Triamnak, R. Yimnirun, J. Pokorny and D. P. Cann, *J. Am. Ceram. Soc.*, 96, 3176–3182 (2013).
14) S. Wada, K. Yamato, P. Pulpan, N. Kumada, B. Y. Lee, T. Iijima, C. Moriyoshi and Y. Kuroiwa, *J. Appl. Phys.*, 108, 094114 (2010).
15) I. Fujii, K. Nakashima, N. Kumada and S. Wada, *J. Ceram. Soc. Japan*, 120, 30–34 (2012).
16) M. C. B. Lopez, G. Fourlaris, B. Rand and F. L. Riley, *J. Am. Ceram. Soc.*, 82, 1777–1786 (1999).
17) S. Aygun, P. Daniels, W. J. Borland and J.-P. Maria, *J. Mater. Res.*, 25, 427–436 (2010).
18) S. Aygun, J. F. Ihlefeld, W. F. Borland and J.-P. Maria, *J. Appl.*

Phys., 109, 034108 (2011).
19) J. A. Voigt, B. A. Tuttle, T. J. Headley and D. L. Lamppa, *Mater. Res. Soc. Symp. Proc.*, 361, 395–402 (1994).
20) A. P. Wilkinson, J. S. Speck, A. K. Cheetham, S. Natarajan and J. M. Thomas, *Chem. Mater.*, 6, 750–754 (1994).
21) G. L. Brennecka, C. M. Parish, B. A. Tuttle, L. N. Brewer and M. A. Rodriguez, *Adv. Mater.*, 20, 1407–1411 (2008).
22) S. L. Swartz and T. R. Shrout, *Mater. Res. Bull.*, 17, 1245–1250 (1982).
23) J. R. Esquivel-Elizondo, B. B. Hinojosa and J. C. Nino, *Chem. Mater.*, 23, 4965–4974 (2011).
24) J. C. Nino, H. J. Young, M. T. Lanagan and C. A. Randall, *J. Mater. Res.*, 17, 1178–1182 (2002).
25) E. M. Levin and R. S. Roth, *J. Res. Natl. Bur. Stand. Sect. A*, 68A, 197–206 (1964).
26) M. L. Barsukova, V. A. Kuznetsov, A. N. Lobachev and Y. V. Shaldin, *J. Cryst. Growth*, 13/14, 530–534 (1972).
27) T. M. Bruton, *J. Solid State Chem.*, 9, 173–175 (1974).
28) J. Ducke, M. Tromel, D. Hohlwein and P. Kizler, *Acta Crystallogr. C*, 52, 1329–1331 (1996).
29) R. S. Roth, *J. Res. Natl. Bur. Stand.*, 56, 17–26 (1956).
30) E. A. Patterson and D. P. Cann, *J. Am. Ceram. Soc.*, 95, 3509–3513 (2012).
31) Q. Zhang, Z. Li, F. Li and Z. Xu, *J. Am. Ceram. Soc.*, 94, 4335–4339 (2011).
32) E. Aksel and J. Jones, *J. Am. Ceram. Soc.*, 93, 3012–3016 (2010).
33) W. Chaisan, R. Yimnirun and S. Ananta, *Ceram. Int.*, 35, 173–176 (2009).
34) A. Beauger, J. C. Mutin and J. C. Niepce, *J. Mater. Sci.*, 18, 3041–3046 (1983).
35) S. Antao and I. Hassan, *Phys. Chem. Miner.*, 34, 573–580 (2007).